REMARKS/ARGUMENTS

In response to the Office Action mailed October 31, 2005, Applicants amend their application and request reconsideration. No claims are added or cancelled so that claims 1-12 remain pending.

Simultaneously with the filing of this Amendment, Applicants are filing an Information Disclosure Statement to bring to the Examiner's attention three publications mentioned in the patent application but not previously supplied by Applicants in any form. At least one of the publications mentioned in the patent application has already been brought to the Examiner's attention in the form of its United States counterparts.

The Examiner asserted that the specification was unclear and provided four examples of alleged lack of clarity. Although Applicants disagree with the Examiner's position, in response to the comments and, particularly, the extensive questions that appear at pages 2-4 of the Office Action, a substitute specification is submitted. In addition to the substitute specification, a computer-generated comparison document showing the differences between the substitute specification and the specification originally filed, i.e., including the changes made by Preliminary Amendment, are attached. No new matter is added in the substitute specification but an attempt has been made to correct minor errors, such as typographical errors, to remove language that is surplusage and potentially confusing, and to conform the text to the conventional mathematical notation that appears within the patent application. The changes made respond to each of the four points raised at page 2 of the Office Action other issues discussed below, and still further issues of clarity not enumerated in the Office Action.

Claims 1-12 were rejected pursuant to 35 USC 112, first paragraph, as not enabled by the description of the patent application. Applicants respectfully disagree with the Examiner's position and respond to the specific points raised in the Office Action as follows.

The Examiner initially questioned the meaning of the terms "n", "I_n", "T_n", "ΔT", "M" and what is meant by the time intervals. The Examiner insisted that an expression appearing at page 8 does not represent an interval but represents a series and suggested

that there is a lack of description of the relationship of the series and time intervals. Further, based upon assumptions made by the Examiner, which do not find support in the disclosure of the patent application, and the misinterpretation of the cited expression as a series, the Examiner insisted that there were inconsistencies in the equations appearing at page 8 of the patent application.

Applicants point out that the term "interval" as employed in the cited passage of the patent application refers to a set of time periods. The term interval does not mean a time separation or length. Because the intervals referred to overlap, as described in the patent application and illustrated in Figure 3, the assumptions made by the Examiner are incorrect. The set of intervals referred to concerns both order and time separation. For example, the interval [a,b] means a mathematical set sometimes represented as $[|x|a \leq x \leq b]$. Since "I_n" means a discrete time, the interval explicitly means a set consisting of the times $(T_n, T_n + \Delta T, \ldots, T_n + (M-1))$.

In a particular example of the invention supplied in the patent application, ΔT is 5 microseconds. "n" is a numerical subscript conventionally used in mathematical notation to denote a sequence of integers, e.g., 0 1, 2.... "M" is a parameter that has an integer value as indicated in the example provided in the patent application. "T_n" is an immediately succeeding time in the recursive formula $T_{n+1} = T_n + (M/(K-1))\,\Delta T$. These basic mathematical concepts are clear to those of ordinary skill in the relevant arts and therefore the disclosure is not confusing or inadequate as to these mathematical elements.

Numerous elements at page 9 of the patent application were likewise questioned. The Examiner prepared, without basis in the patent application, his own definition of ΔT and asserted that the equation on page 9 in line 5 is inconsistent with that "common" definition. Of course, every applicant has the right to define his own terms in his patent application and it is those terms that must be given consideration in the examination process, not a definition outside the specification and suggested by the Examiner.

With regard to the specific questions, "M" was already pointed out as being an integer parameter that, in the specific example provided in the patent application, is 256. Likewise "K" is another parameter that, in the specific example is 8. The meaning of the

term ΔT has already been explained in terms of the recursive formula. There is no contradiction in the cited passages at page 9 of the patent application.

The Examiner further questioned the term "Hanning window of the order M," questioning whether the M is the same as defined elsewhere in the specification. The definition of a Hanning window is provided in the equation (1) of the patent application and is a term well known in the signal processing arts. Proof of this knowledge is supplied by Oppenheim et al., *Discrete-Time Signal Processing* (1989) at pages 447 - 449. A copy of this excerpt from Oppenheim is attached. In addition, attention is directed to page 4 of an eight-page attachment from the Wikipedia. "M" is used consistently throughout the patent application.

The foregoing comments provide answers to the questions that appear beginning in the final two lines at page 3 of the Office Action and carrying over to the first two lines of page 4.

The Examiner questioned the statement appearing at page 10 in lines 9 and 10 of the original specification, stating that the logical expression f(x) becomes a true value. As well known to those versed in the mathematical arts, a logical expression or formula provides either a true or false answer depending upon whether the formula is satisfied. As an example, with respect to a sequence {n(0), a(1), ... a(100)}, the expression $\Sigma_{[1\leq x\leq 2]}$ {a(x)} means a sum of sequences with respect to x. Thus, this expression establishes whether a logical formula $1 \leq x \leq 2$ has a true value, i.e., a(1) + a(2) is correct, i.e., takes on a true value, or, if not satisfied, is false.

In the substitute specification, the "standard factor C" is changed to a "standardizing" factor for clarity. The Examiner asserts that this factor should be a function of "n" and Applicants agree. This error in Equation 4 is regretted and is corrected in the substitute specification.

The comment regarding a "resolution" principle on page 12 of the original specification was questioned. The term reflects a minor translational error. At that point in the patent application reference is being made to the resistance to electrical impulse noise of the invention in detecting knocking in an internal combustion engine by

detecting changes in ion current. The translational error is corrected in the substitute specification.

The Examiner questioned the term appearing at page 13 of the original patent application, "Gabor wavelet component", pointing out that this term is not defined in the patent application. Of course, it is not necessary to define in a patent application a term well known to those of ordinary skill in the relevant arts. As one example of knowledge concerning a Gabor wavelet, enclosed is a passage and corresponding English language translation from a Japanese language publication by Nakano et al., *Signal Processing and Imaging Processing by Wavelet* (1999). Further, much more information concerning both the Hanning window and the Gabor wavelet can be obtained simply by entering each of those terms in an Internet search.

Finally, the term "L" in equation 6 appearing on page 13 of the patent application was also questioned. Like other questioned symbols, "L" represents is a parameter and examples of values of that parameter are supplied at page 13 of the patent application.

The foregoing comments establish that the disclosure of the patent application would be understood by a person of ordinary skill in the relevant arts and that, therefore, the disclosure of the patent application is enabling, meeting the requirements of 35 USC 112, first paragraph.

Claims 1, 2, 4, 7, 8, 10, and 11 were rejected as anticipated by Frankowski et al. (U.S. Patent 6,456,927, hereinafter Frankowski). It is understood that claim 5 is similarly rejected because it is mentioned in the same section of the Office Action with the rejection of the other claims listed there. Claims 6 and 12 were rejected as obvious over Frankowski considered by itself. Presumably, there was no prior art rejection of claims 3 and 9, only a rejection of those claims as not enabled. The prior art rejections are respectfully traversed.

In order to anticipate any claim, a prior art publication must disclose every element of the claimed invention. If Frankowski fails to disclose every element of the two pending independent claims, claims 1 and 7, then it cannot anticipate, nor by itself, make any pending claim obvious.

Frankowski, like the invention, is directed to detecting knocking in an internal combustion engine. However, the similarity between the disclosed and claimed invention and Frankowski ends at that point. Although Frankowski is particularly directed to identifying knocking by analyzing mechanical vibration signals there is a reference in column 4 in the paragraph beginning in line 50 to use of other sensors in detecting knocking. Reference is made to optical, in-cylinder pressure, and flame ionization sensor technologies. That paragraph emphasizes the use of an accelerometer as the preferred sensor and points out that the accelerometer measures mechanical vibrations.

The present invention, in the apparatus claim 1, requires the use of an ion current detecting means. In the method of claim 7, ion currents are detected using the spark plugs of the internal combustion engine. Frankowski never describes sensing ion currents nor processing electrical signals based upon ion currents to detect the presence of knocking in an internal combustion engine. The reference to a flame ionization sensor is not a reference to a measurement of ion current or an ion current sensor as in the present invention. A flame ionization sensor measures ionization attributable to flames within a cylinder of an internal combustion engine. No such sensor is employed in the invention. Instead, ion currents are sensed directly through the spark plugs of the internal combustion engine. Because of at least that difference, Frankowski cannot anticipate any pending claim nor make any pending claim obvious. Of course, there are substantial additional differences between Frankowski and the claimed invention with regard to signal processing but description of those additional differences is not required at the present time to distinguish the invention from Frankowski.

Further, Frankowski could not be applied, as in the present invention, to extract signals from electrodes of the spark plug that could be processed, according to Frankowski's disclosure, to detect knocking. An ignition signal applied or sensed at a spark plug has an energy at least one million times larger than the energy of a flame ionization signal from a flame ionization sensor. If Frankowski's flame ionization signal processing apparatus were directly connected to spark plugs, as in the invention, Frankowski's circuitry, particularly the analog-to-digital converter, would the destroyed

because of the strength of the input signal. This effect further demonstrates that the invention presently claimed cannot be even suggested by Frankowski.

Reconsideration and allowance of claims 1-12 are earnestly solicited.

Respectfully submitted,

Jeffrey A. Wyand, Reg. No. 29,458
LEYDIG, VOIT & MAYER
700 Thirteenth Street, N.W., Suite 300
Washington, DC 20005-3960
(202) 737-6770 (telephone)
(202) 737-6776 (facsimile)

Date: February 28, 2006
JAW:ves

Original copy

"Signal processing and image processing by wavelet" written by Nakano et al. (Kyoritsu Shuppan Ltd. 1999) pp. 38-39

2.2.2　ガボールウェーブレットの定義

この節では，窓フーリエ変換で利用されるガボール関数から，連続ウェーブレットの一種であるガボールウェーブレットを構成する方法を説明する．ガボール関数は次式のように定義されている．

$$G^{\alpha}_{b,\omega_0}(t) = e^{i\omega_0 t} g_\alpha(t-b) \tag{2.15}$$

ここで窓関数 $g_\alpha(t)$ は，積分値が1に規格化されたガウス関数で，

$$g_\alpha(t) = \frac{1}{2\sqrt{\pi\alpha}} e^{-\frac{t^2}{4\alpha}} \tag{2.16}$$

である．α はガウス窓の幅を示す指数であり，b は時間軸のシフトの量を示すものである．また，ω_0 は，振動の中心周波数である．ところで，ガボール関数は，式(2.15)を見るとわかるように，b の変化に応じて関数の形が相似でなくなる．これは，ガウス窓の中心座標は b の変化に伴って時間軸をシフトするが，$e^{i\omega_0 t}$ は b に依存しないからである．この性質は，シフトおよびダイレーション（拡大縮小）を行っても，関数の形が相似であるというウェーブレットの性質にそぐわない．そこで，式(2.15)において，$b=0$ として次のように原点で $\psi(t)$ を定義する．

$$\psi(t) = g_\sigma(t) e^{i\omega_0 t} \tag{2.17}$$

ここで窓関数 $g_\sigma(t)$ は，式(2.16)と異なり，

$$g_\sigma(t) = \frac{1}{2\sqrt{\pi\sigma}} e^{-\frac{t^2}{4\sigma^2}} \tag{2.18}$$

で定義される．この g_σ は，σ によらずガウス関数の2乗積分値が一定である．これは，式(2.9)において，ダイレーションによらずウェーブレットの2乗積分値が一定であることと対応している．

式(2.17)において，式(2.9)と同様 $t=(t-b)/a$ とすれば，シフトとダイレーションによって関数の形が相似となるので，ウェーブレットを形成する．これを基底としたウェーブレット変換をガボール ウェーブレット変換 (Gabor wavelet transform) と呼ぼう．

ところで，前述したウェーブレットの再構成条件を満たすには，この逆変換が存在しなければならない．このため，関数 ψ の直流成分が0，すなわち，

そのフーリエ変換において，$\widehat{\psi}(0)=0$ であることが必要である．そこで，これを達成するために式(2.17)の ψ を次のように再定義する．

$$\psi(t)=g_\sigma(t)\left[e^{i\omega_0 t}-e^{-(\sigma\omega_0)^2}\right] \tag{2.19}$$

上式のフーリエ変換は，

$$\begin{aligned}\widehat{\psi}(\omega)&=\int_{-\infty}^{\infty}g_\sigma(t)[e^{i\omega_0 t}-e^{-(\sigma\omega_0)^2}]e^{-i\omega t}dt\\&=\int_{-\infty}^{\infty}g_\sigma(t)e^{-i(\omega-\omega_0)t}dt-e^{-(\sigma\omega_0)^2}\int_{-\infty}^{\infty}g_\sigma(t)e^{-i\omega t}dt\end{aligned} \tag{2.20}$$

ここで，積分公式

$$\int_{-\infty}^{\infty}e^{-i\omega t}e^{-at^2}dt=\sqrt{\frac{\pi}{a}}e^{\frac{-\omega^2}{4a}} \tag{2.21}$$

より，

$$\widehat{\psi}(\omega)=\sqrt{\sigma}\left(e^{-\sigma^2(\omega-\omega_0)^2}-e^{-\sigma^2(\omega^2+\omega_0^2)}\right) \tag{2.22}$$

この式で $\omega=0$ として次式をえる．

$$\widehat{\psi}(0)=0 \tag{2.23}$$

つまり，直流成分が，σ および ω_0 によらず0であることがわかる．図2.19に，$\sigma=5$, $\omega_0=\pi/4$, $b=20$ のときのガボール ウェーブレットの実部と虚部を示す．ガボール ウェーブレット $\psi(t)$ は，その基底に正弦波成分を含んでいるので，時間的に局在する周期的な波形の解析に有効である．

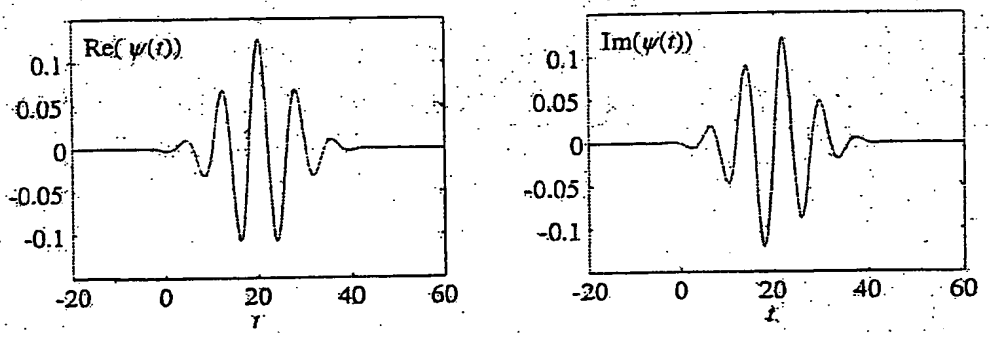

(a) 実部　　(b) 虚部

図 2.19　ガボール ウェーブレットの実部 (a) と虚部 (b)

"Signal processing and image processing by wavelet" written by Nakano et al. (Kyoritsu Shuppan Ltd. 1999) pp. 38-39

Chapter 2 Window fourie transform and wavelet transform of signal

2.2 Continuous wavelet transform

2.2.2 Definition of Gabor wavelet

In this paragraph, a method for constructing the Gabor wavelet which is one of the continuous wavelets based on the Gabor function which is used in the window Fourier transform is explained. The Gabor function is defined by a following formula.

$$G^{\alpha}_{b,\omega_0}(t) = e^{i\omega_0 t} g_{\alpha}(t-b) \tag{2.15}$$

Here, the window function $g_\alpha(t)$ is expressed by the Gauss function standardized with an integrated value of 1 as follows.

$$g_{\alpha}(t) = \frac{1}{2\sqrt{\pi\alpha}} e^{-\frac{t^2}{4\alpha}} \tag{2.16}$$

Here, α is an exponent which indicates a width of the Gauss window, and b indicates a quantity of shift on a time axis. Further, ω_0 indicates the center frequency of vibrations. Here, in the Gabor function, as can be understood from the formula (2.15), the function does not hold the similar shape along with the change of b. This is because that although the center coordinates of the Gauss window is shifted on a time axis along with the change of b, $e^{i\omega 0t}$ does not depend on b. This property does not conform with the property of wavelet that the shape of the function is held in a similar shape even when the shift or the dilation (enlargement or shrinkage) is conducted. Accordingly, provided that b=0, in the formula (2.15), ψ (t) is defined as follows at an origin.

$$\psi(t) = g_{\sigma}(t) e^{i\omega_0 t} \tag{2.17}$$

Here, the window function $g_\sigma(t)$ is, different from the formula (2.16), defined as follows.

$$g_{\sigma}(t) = \frac{1}{2\sqrt{\pi\sigma}} e^{-\frac{t^2}{4\sigma^2}} \tag{2.18}$$

With respect to g_σ, a square integrated value of the Gauss function is fixed irrespective of σ. This corresponds to a fact that a square integrated value of wavelet is fixed irrespective of the dilation in the formula (2.9).

In the formula (2.17), by assuming t as t=(t-b)/a in the same manner as the formula (2.9), the shape of the function becomes similar due to the

shift and the dilation and hence, the wavelet is formed. The wavelet transform which uses the wavelet as a basis is referred to as the Gabor wavelet transform.

Here, to satisfy the above-mentioned reconstructing conditions of the wavelet, it is inevitable that the inverted transform exists. For this end, it is necessary that a direct current component of the function ψ is 0, that is, in the Fourier transform thereof, $\psi(0)=0$. Accordingly, to achieve this, ψ in the formula (2.17) is redefined as follows.

$$\psi(t) = g_\sigma(t)\left[e^{i\omega_0 t} - e^{-(\sigma\omega_0)^2}\right] \tag{2.19}$$

The Fourier transform in the above-mentioned formula is expressed as follows.

$$\begin{aligned}\widehat{\psi}(\omega) &= \int_{-\infty}^{\infty} g_\sigma(t)[e^{i\omega_0 t} - e^{-(\sigma\omega_0)^2}]e^{-i\omega t}dt \\ &= \int_{-\infty}^{\infty} g_\sigma(t)e^{-i(\omega-\omega_0)t}dt - e^{-(\sigma\omega_0)^2}\int_{-\infty}^{\infty} g_\sigma(t)e^{-i\omega t}dt \end{aligned} \tag{2.20}$$

Here, due to an integral formula,

$$\int_{-\infty}^{\infty} e^{-i\omega t}e^{-at^2}dt = \sqrt{\frac{\pi}{a}}e^{\frac{-\omega^2}{4a}} \tag{2.21}$$

$$\widehat{\psi}(\omega) = \sqrt{\sigma}\left(e^{-\sigma^2(\omega-\omega_0)^2} - e^{-\sigma^2(\omega^2+\omega_0^2)}\right) \tag{2.22}$$

by setting ω as $\omega=0$, a following formula is obtained.

$$\widehat{\psi}(0) = 0 \tag{2.23}$$

That is, it is understood that the direct current component is 0 irrespective of σ and ω_0. Fig. 2.19 shows a real part and an imaginary part of the Gabor wavelet when $\sigma=5$, $\omega_0=\pi/4$ and b=20. Since the Gabor wavelet $\psi(t)$ includes a sinusoidal component in a basis thereof, the Gabor wavelet $\psi(t)$ is effective in analyzing the periodical waveform which locally exists with time.

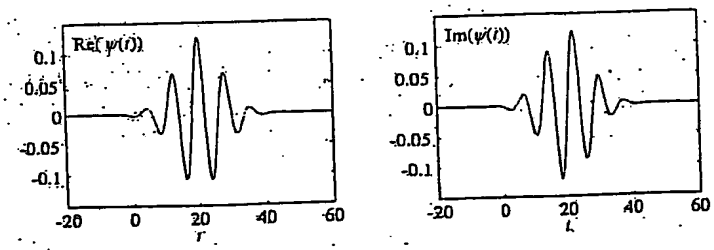

Fig. 2.19 real part and imaginary part of Gabor wavelet
(a) real part (b) imaginary part

Window function

From Wikipedia, the free encyclopedia
(Redirected from Hanning window)

In signal processing, a **window function** (or **apodization function**) is a function that is zero-valued outside of some chosen interval. For instance, a function that is constant inside the interval and zero elsewhere is called a **rectangular window**, which describes the shape of its graphical representation. When another function or a signal (data) is multiplied by a window function, the product is also zero-valued outside the interval. All that is left is the "view" through the window. Applications of window functions include spectral analysis and filter design.

Contents

Spectral analysis

It can be shown theoretically that the Fourier transform of the function: $\cos(\omega t)$ is zero, except right at frequency ω. But many other functions and data (that is, *waveforms*) do not have convenient closed form transforms. Or we might be interested in their spectral content only during a certain time period. In either case, we have to perform the Fourier transform (or something similar) on one or more finite intervals of the waveform. So in general, the transform is applied to the product of the waveform and a window function. But any window (including rectangular) affects the spectrum that we are trying to measure.

The effect is easiest to understand in terms of a simple waveform, like $\cos(\omega t)$. Windowing causes its Fourier transform to have non-zero values (commonly called **leakage**) at frequencies other than ω. It tends to be worst (highest) near ω and least at frequencies farthest from ω. If there are two sinusoids,

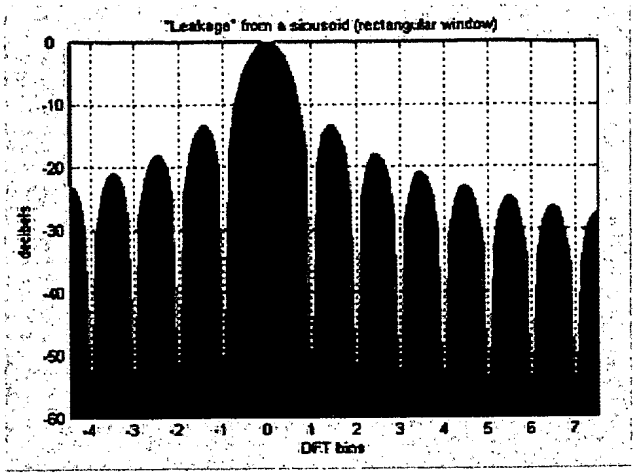

Zoom view of spectral leakage

with different frequencies, leakage can interfere with our ability to distinguish them spectrally. If their frequencies are dissimilar, then the leakage interferes when one sinusoid is much smaller in amplitude than the other. That is its spectral component can be hidden by the leakage from the larger component. But when the frequencies are near each other, the leakage can be sufficient to interfere even when the sinusoids are equal strength. I.e., they become *unresolvable*. The rectangular window has excellent resolution characteristics for signals of comparable strength, but it is a poor choice for signals of disparate amplitudes. This characteristic is sometimes described as *low dynamic range*. At the other extreme of dynamic range are the windows with the poorest resolution. And they are also poorest in terms of ***sensitivity***. I.e., if the input waveform contains random noise, its spectral amplitude, compared to the sinusoid, will appear higher than with a less extreme window. In other words, the ability to find weak sinusoids amidst the noise is diminished by a high dynamic range window. High dynamic range windows are probably most-often justified in *wideband applications*, where the spectrum being analyzed is expected to contain many different signals of various strengths.

In between the extremes are moderate windows, such as Hamming and Hann. They are commonly used in *narrowband applications*, such as the spectrum of a telephone channel. In summary, spectral analysis involves a tradeoff between resolving comparable strength signals with similar frequencies and resolving disparate strength signals with dissimilar frequencies. That tradeoff occurs when the window function is chosen.

Discrete-time signals

When the input waveform is time-sampled, instead of continuous, the analysis is usually done by applying a window function and then a discrete Fourier transform (DFT). But the DFT provides only a coarse sampling of the actual DTFT spectrum. The figure above shows a portion of the DTFT for a rectangularly-windowed sinusoid. The actual frequency of the sinusoid is indicated as "0" on the horizontal axis. Everything else is leakage. The unit of frequency is "DFT bins"; that is the integer values are the frequencies sampled by the DFT. So the figure depicts a case where the actual frequency of the sinusoid happens to coincide with a DFT sample, and the maximum value of the spectrum is accurately measured by that sample. When it misses the maximum value by some amount [up to 1/2 bin], the measurement error is referred to as ***scalloping loss*** (inspired by the shape of the peak). But the most interesting thing about this case is that all the other samples coincide with **nulls** in the true spectrum. (The nulls are actually zero-crossings, which cannot be shown on a logarithmic scale such as this.) So in this case, the DFT creates the **illusion** of no leakage. Despite the unlikely conditions of this example, it is a popular misconception that visible leakage is some sort of artifact of the DFT. But since any window function causes leakage, its apparent absence (in this contrived example) is actually the DFT artifact.

Total leakage

The concepts of resolution and dynamic range tend to be somewhat subjective, depending on what the user is actually trying to do. But they also tend to be highly correlated with the total leakage, which is quantifiable. It is usually expressed as an equivalent bandwidth, B. Think of it as redistributing the DTFT into a rectangular shape with height equal to the spectral maximum and width B. The more leakage, the greater the bandwidth. It is sometimes called *noise equivalent bandwidth* or *equivalent noise bandwidth*.

Although we have depicted leakage as interference that one component imposes on other frequencies, the

effect is reciprocal. Thus, if frequency f_1 leaks a percentage of its energy into frequency f_2, then a frequency component at f_2 returns the favor in the same proportion, as does every other frequency component of the input signal in varying amounts. So the spectral measurement at frequency f_1 is perturbed by all the other components. The greater the noise bandwidth (B), the greater the effect.

Processing gain

In signal processing, operations are chosen to improve some aspect of quality of a signal by exploiting the differences between the signal and the corrupting influences. When the signal is a sinusoid corrupted by additive random noise, spectral analysis distributes the signal and noise components differently, often making it easier to detect the signal's presence or measure certain characteristics, such as amplitude and frequency. Effectively, the signal to noise ratio (SNR) is improved by distributing the noise uniformly, while concentrating most of the sinusoid's energy around one frequency. *Processing gain* is a term often used to describe an SNR improvement. The processing gain of spectral analysis depends on the window function, both its noise bandwidth (B) and its potential scalloping loss. These effects partially offset, because windows with the least scalloping naturally have the most leakage.

For example, the worst possible scalloping loss from a Blackman-Harris window (below) is 0.83 dB, compared to 1.42 dB for a Hann window. But the noise bandwidth is larger by a factor of 2.01/1.5, which can be expressed in decibels as: $10 \log_{10}(2.01 / 1.5) = 1.27$. Therefore, even at maximum scalloping, the net processing gain of a Hann window exceeds that of a Blackman-Harris window by: 1.27 +0.83 -1.42 = 0.68 dB. And when we happen to incur no scalloping (due to a fortuitous signal frequency), the Hann window is 1.27 dB more *sensitive* than Blackman-Harris. In general (as mentioned earlier), this is a deterrent to using high-dynamic range windows in low-dynamic range applications.

Window examples

Terminology:

- N represents the width, in samples, of a discrete-time window function. Typically it is an integer power-of-2, such as $2^{10} = 1024$.
- n is an integer, with values $0 \leq n \leq N - 1$. So these are the time-shifted forms of the windows: $w(n - \frac{N-1}{2})$, where $w(n)$ is maximum at $n = 0$.
  - Some of these forms have an overall width of $N-1$, which makes them zero-valued at $n=0$ and $n=N-1$. That sacrifices two data samples for no apparent gain, if the DFT size is N. When that happens, an alternative approach is to replace $N-1$ with N in the formula.
- Each figure label includes the corresponding noise equivalent bandwidth metric (B), in units of *DFT bins*. As a guideline, windows are divided into two groups on the basis of B. One group comprises $1 \leq B \leq 1.8$, and the other group comprises $B \geq 1.98$. The Gauss and Kaiser windows are families that span both groups, though only one or two examples of each are shown.

High- and moderate-resolution windows

Rectangular window

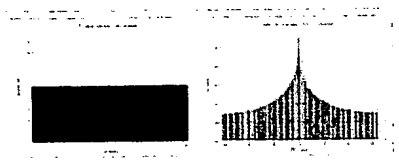

Rectangular window; B=1.00

$$w(n) = 1$$

Gauss windows

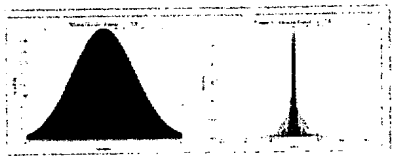

Gauss window, σ=0.4; B=1.45

$$w(n) = e^{-\frac{1}{2}\left(\frac{n-(N-1)/2}{\sigma(N-1)/2}\right)^2}$$

$$\sigma \leq 0.5$$

Hamming window

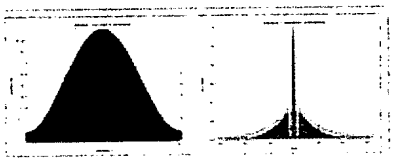

Hamming window; B=1.37

$$w(n) = 0.53836 - 0.46164 \cos\left(\frac{2\pi n}{N-1}\right)$$

Hann window

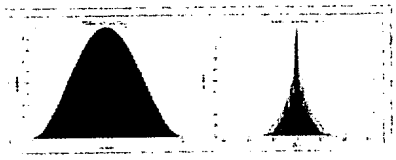

Hann window; B=1.50

$$w(n) = 0.5 \left(1 - \cos\left(\frac{2\pi n}{N-1}\right)\right)$$

The Hann window is sometimes called the "Hanning" window, in analogy to the Hamming window. However, this is incorrect, because the windows were named after Julius von Hann and Richard Hamming, respectively.

Bartlett window (zero valued end-points)

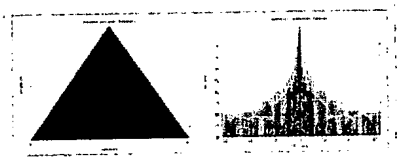

Bartlett window; B=1.33

$$w(n) = \frac{N-1}{2} - \left| n - \frac{N-1}{2} \right|$$

Triangular window (non-zero end-points)

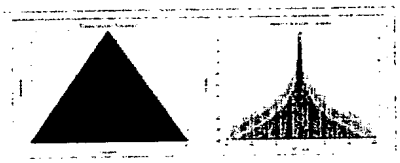

Triangular window; B=1.33

$$w(n) = \frac{N}{2} - \left| n - \frac{N-1}{2} \right|$$

Bartlett-Hann window

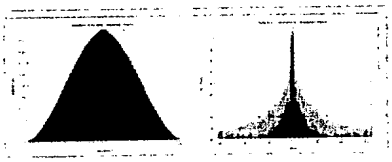

Bartlett-Hann window; B=1.46

$$w(n) = a_0 - a_1 \left| \frac{n}{N-1} - \frac{1}{2} \right| - a_2 \cos\left(\frac{2\pi n}{N-1}\right)$$

$$a_0 = 0.62; \quad a_1 = 0.48; \quad a_2 = 0.38$$

Blackman window

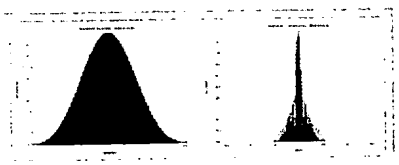

Blackman window; B=1.73

$$w(n) = a_0 - a_1 \cos\left(\frac{2\pi n}{N-1}\right) + a_2 \cos\left(\frac{4\pi n}{N-1}\right)$$

$$a_0 = 0.42; \quad a_1 = 0.5; \quad a_2 = 0.08$$

Kaiser windows

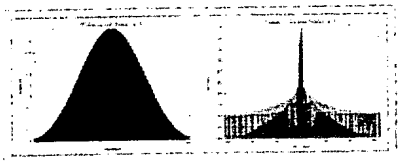

Kaiser window, α =2; B=1.50

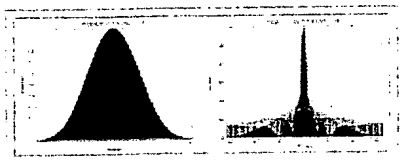

Kaiser window, α =3; B=1.80

$$w(n) = \frac{I_0\left(\pi\alpha\sqrt{1-(\frac{2n}{N-1}-1)^2}\right)}{I_0(\pi\alpha)}$$

See Kaiser window.

Low-resolution (high dynamic range) windows

Nuttall window, continuous first derivative

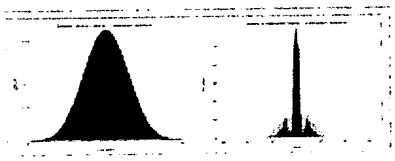

Nuttall window, continuous first derivative; B=2.02

$$w(n) = a_0 - a_1\cos\left(\frac{2\pi n}{N-1}\right) + a_2\cos\left(\frac{4\pi n}{N-1}\right) - a_3\cos\left(\frac{6\pi n}{N-1}\right)$$

$$a_0 = 0.355768; \quad a_1 = 0.487396; \quad a_2 = 0.144232; \quad a_3 = 0.012604$$

Blackman-Harris window

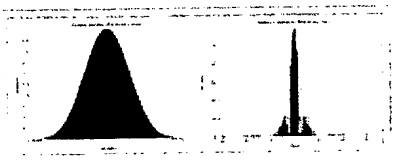

Blackman-Harris window; B=2.01

$$w(n) = a_0 - a_1\cos\left(\frac{2\pi n}{N-1}\right) + a_2\cos\left(\frac{4\pi n}{N-1}\right) - a_3\cos\left(\frac{6\pi n}{N-1}\right)$$

$$a_0 = 0.35875; \quad a_1 = 0.48829; \quad a_2 = 0.14128; \quad a_3 = 0.01168$$

Blackman-Nuttall window

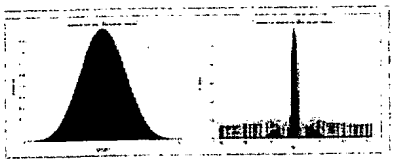

Blackman-Nuttall window; B=1.98

$$w(n) = a_0 - a_1 \cos\left(\frac{2\pi n}{N-1}\right) + a_2 \cos\left(\frac{4\pi n}{N-1}\right) - a_3 \cos\left(\frac{6\pi n}{N-1}\right)$$

$$a_0 = 0.3635819; \quad a_1 = 0.4891775; \quad a_2 = 0.1365995; \quad a_3 = 0.0106411$$

Flat top window

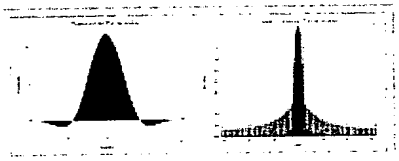

Flat top window; B=3.77

$$w(n) = a_0 - a_1 \cos\left(\frac{2\pi n}{N-1}\right) + a_2 \cos\left(\frac{4\pi n}{N-1}\right) - a_3 \cos\left(\frac{6\pi n}{N-1}\right) + a_4 \cos\left(\right.$$

$$a_0 = 1; \quad a_1 = 1.93; \quad a_2 = 1.29; \quad a_3 = 0.388; \quad a_4 = 0.032$$

Other windows

Bessel window

Sine window

Multiple overlap windows

When using FFT or DCT for spectral analysis a sample belongs to **one** analysis window. When using windowing, samples at the boundaries are attenuated.

To reduce the effect that these samples become less important for the result, normally windows are overlapped. So samples between two blocks are attenuated, but they belong to two blocks: their influence is still (nearly) the same as samples which are not attenuated. But it is possible to overlap more than two windows. This typically makes the transition band between main slope and side slopes smaller.

Triple overlapped cosine window

The normal cosine windows do not preserve the power of the signal. Samples which are exactly between two blocks are attenuated by 6 dB, i.e., their power is reduced by a factor of 0.25. The overlapping reduces this to

a factor of 0.5.

References

- Oppenheim, A.V., and R.W. Schafer, *Discrete-Time Signal Processing*, Upper Saddle River, NJ: Prentice-Hall, 1999, pp 468-471.
- Albert H. Nuttall, *Some Windows with Very Good Sidelobe Behavior*, IEEE Transactions on Acoustics, Speech, and Signal Processing, Vol.ASSP-29, No.1, February 1981, pp 84-91.
- Frederic J. Harris, *On the use of Windows for Harmonic Analysis with the Discrete Fourier Transform*, Proceedings of the IEEE, Vol.66, No.1, January 1978, pp 51-83.

Categories: Statistics | Fourier analysis | Signal processing | Digital signal processing

Discrete-Time Signal Processing

Alan V. Oppenheim
Ronald W. Schafer

PRENTICE HALL, Englewood Cliffs, New Jersey 07632

Library of Congress Cataloging-in-Publication Data

Oppenheim, Alan V.
Discrete-time signal processing / Alan V. Oppenheim, Ronald W. Schafer.
p. cm.—(Prentice Hall signal processing series)
Bibliography: p.
Includes index.
ISBN 0-13-216292-X
1. Signal processing—Mathematics. 2. Discrete-time systems.
I. Schafer, Ronald W. II. Title. III. Series.
TK5102.5.02452 1989
621.38'043—dc 19 88-25562
CIP

Editorial/production supervision: Barbara G. Flanagan
Interior design: Roger Brower
Cover design: Vivian Berman
Manufacturing buyer: Mary Noonan

Published by Prentice-Hall, Inc.
A Division of Simon & Schuster
Englewood Cliffs, New Jersey 07632

Printed in the United States of America
10 9 8 7 6 5 4 3

ISBN 0-13-216292-X

Prentice-Hall International (UK) Limited, *London*
Prentice-Hall of Australia Pty. Limited, *Sydney*
Prentice-Hall Canada Inc., *Toronto*
Prentice-Hall Hispanoamericana, S.A., *Mexico*
Prentice-Hall of India Private Limited, *New Delhi*
Prentice-Hall of Japan, Inc., *Tokyo*
Simon & Schuster Asia Pte. Ltd., *Singapore*
Editora Prentice-Hall do Brasil, Ltda., *Rio de Janeiro*

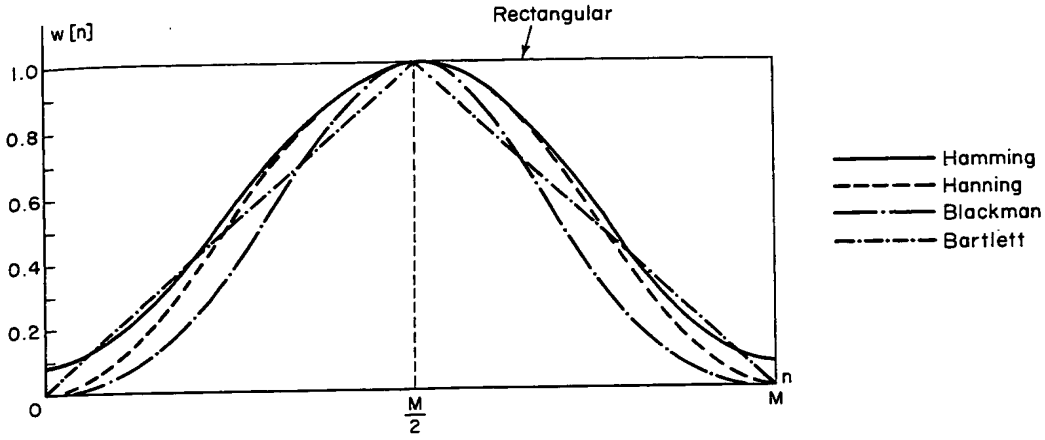

Figure 7.29 Commonly used windows.

7.4.1 Properties of Commonly Used Windows

Some commonly used windows are shown in Fig. 7.29.† These windows are defined by the following equations:

Rectangular

$$w[n] = \begin{cases} 1, & 0 \le n \le M, \\ 0, & \text{otherwise} \end{cases} \tag{7.77a}$$

Bartlett (triangular)

$$w[n] = \begin{cases} 2n/M, & 0 \le n \le M/2, \\ 2 - 2n/M, & M/2 < n \le M, \\ 0, & \text{otherwise} \end{cases} \tag{7.77b}$$

Hanning

$$w[n] = \begin{cases} 0.5 - 0.5\cos(2\pi n/M), & 0 \le n \le M, \\ 0, & \text{otherwise} \end{cases} \tag{7.77c}$$

Hamming

$$w[n] = \begin{cases} 0.54 - 0.46\cos(2\pi n/M), & 0 \le n \le M, \\ 0, & \text{otherwise} \end{cases} \tag{7.77d}$$

† The Bartlett, Hanning, Hamming, and Blackman windows are all named after their originators. The Hanning window is associated with Julius von Hann, an Austrian meteorologist, and is sometimes referred to as the Hann window. The term "hanning" was used by Blackman and Tukey (1958) to describe the operation of applying this window to a signal and has since become the most widely used name for the window, with varying preferences for the choice of "Hanning" or "hanning."

Blackman

$$w[n] = \begin{cases} 0.42 - 0.5\cos(2\pi n/M) + 0.08\cos(4\pi n/M), & 0 \le n \le M, \\ 0, & \text{otherwise} \end{cases} \quad (7.77e)$$

(For convenience, Fig. 7.29 shows these windows plotted as functions of a continuous variable; however, as specified in Eqs. 7.77, the window sequence is defined only at integer values of n.)

As will be discussed in Chapter 11, the windows defined in Eqs. (7.77) are commonly used for spectrum analysis as well as FIR filter design. They have the desired property that their Fourier transforms are concentrated around $\omega = 0$, and they have a simple functional form that allows them to be computed easily. The Fourier transform of the Bartlett window can be expressed as a product of Fourier transforms of rectangular windows, and the Fourier transforms of the other windows can be expressed as sums of frequency-shifted Fourier transforms of the rectangular window as given by Eq. (7.76). (See Problem 7.25.)

The function $20\log_{10}|W(e^{j\omega})|$ is plotted in Fig. 7.30 for each of these windows with $M = 50$. The rectangular window clearly has the narrowest mainlobe and thus, for a given length, it should yield the sharpest transitions of $H(e^{j\omega})$ at a discontinuity of $H_d(e^{j\omega})$. However, the first sidelobe is only about 13 dB below the main peak, resulting in oscillations of $H(e^{j\omega})$ of considerable size around discontinuities of $H_d(e^{j\omega})$. Table 7.2, which compares the windows of Eqs. (7.77), clearly shows that by

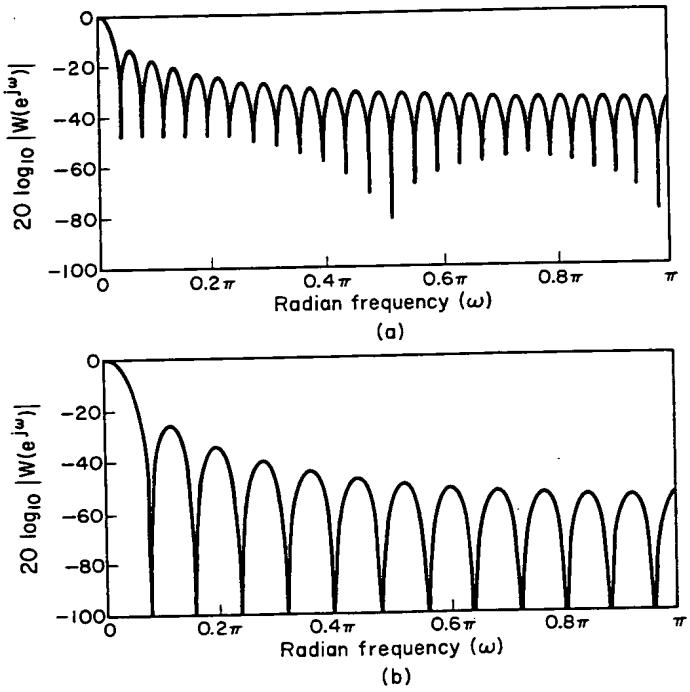

Figure 7.30 Fourier transforms (log magnitude) of windows of Fig. 7.29. (a) Rectangular. (b) Bartlett.

$$0 \le n \le M, \quad \text{otherwise} \qquad (7.77e)$$

ted as functions of a window sequence is

ied in Eqs. (7.77) are lesign. They have the ed around $\omega = 0$, and computed easily. The ; a product of Fourier s of the other windows rms of the rectangular

each of these windows 'est mainlobe and thus, $(e^{j\omega})$ at a discontinuity below the main peak, und discontinuities of), clearly shows that by

Fig. 7.29. (a) Rectan-

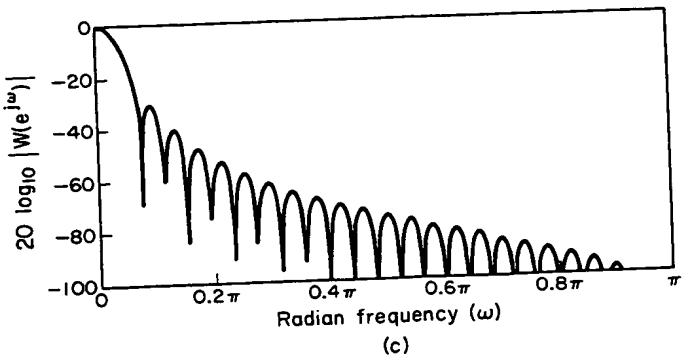

(c)

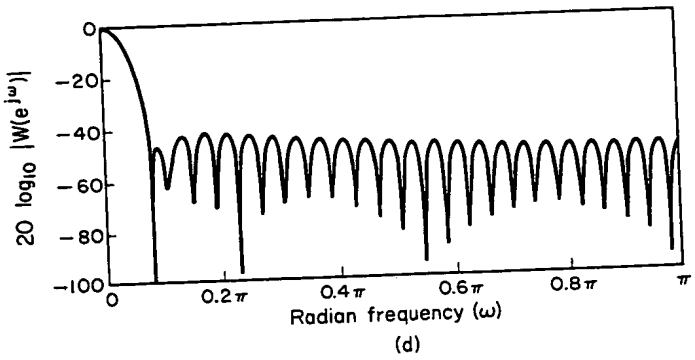

(d)

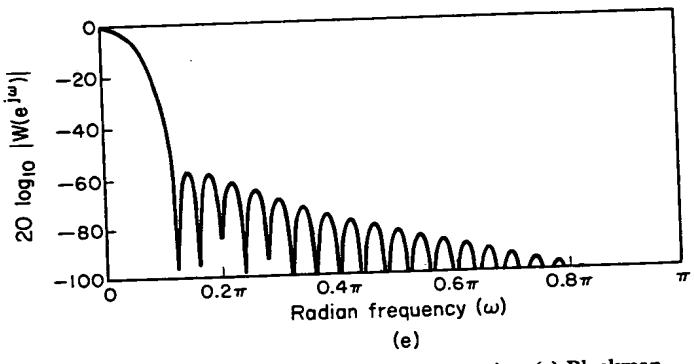

(e)

Figure 7.30 (*continued*) (c) Hanning. (d) Hamming. (e) Blackman.

tapering the window smoothly to zero as with the Hamming, Hanning, and Blackman windows, the sidelobes (second column) are greatly reduced; however, the price paid is a much wider mainlobe (third column) and thus wider transitions at discontinuities of $H_d(e^{j\omega})$. The other columns of Table 7.2 will be discussed later.

7.4.2 Incorporation of Generalized Linear Phase

In designing many types of FIR filters, it is desirable to obtain causal systems with generalized linear phase response. All the windows of Eqs. (7.77) have been defined in